Contribution from the Chemistry Department,
University of Hawaii, Honolulu, Hawaii 96822

Crystal and Molecular Structure of (2,9-Dimethyl-1,10-phenanthroline)(glycylglycinato)copper(II) Pentahydrate

CHARLES J. SIMMONS, MUNIME LUNDEEN, and KARL SEFF*

Received November 9, 1977

The crystal and molecular structure of (2,9-dimethyl-1,10-phenanthroline)(glycylglycinato)copper(II) pentahydrate, $CuC_{18}H_{18}N_4O_3\cdot 5H_2O$, has been determined by single-crystal x-ray diffraction techniques using the 4030 unique and significant (at the 2σ level) reflections for which $2\theta < 55°$ and was refined by full-matrix least-squares procedures to a final conventional R index of 0.038. Counter methods and monochromatized Mo Kα radiation were employed. The complex crystallizes in the monoclinic space group $P2_1/c$, with $a = 9.591$ (4) Å, $b = 14.478$ (3) Å, $c = 17.238$ (5) Å, and $\beta = 114.79$ (2)° and with four molecules per unit cell. In this mixed-ligand Cu(II) complex, glycylglycinato serves as a tridentate ligand, coordinating with its amino nitrogen (Cu–N, 2.050 (2) Å), ionized amide nitrogen (Cu–N, 1.900 (2) Å), and carboxylate oxygen (Cu–O, 2.033 (2) Å) donor atoms. A fourth position, completing a distorted square about Cu(II), is occupied by one of the two dimethylphenanthroline nitrogen atoms (Cu–N, 2.013 (2) Å), while the other nitrogen occupies a near-apical position at a somewhat longer coordination distance (Cu–N, 2.263 (2) Å). The geometry about Cu(II) is five-coordinate distorted square pyramidal. The compound was prepared by reacting copper(II) perchlorate with glycylglycine and 2,9-dimethyl-1,10-phenanthroline in basic solution. It has an intense absorption at 633 nm (ϵ 313), in contrast to most other copper(II)–simple peptide complexes, whose extinction coefficients are approximately 100 or less in the visible region. The EPR parameters of frozen solutions of the compound are $g_{\parallel} = 2.230$, $g_{\perp} = 2.064$, and $|A_{\parallel}| = 16.3 \times 10^{-3}$ cm^{-1}.

Introduction

There has been some interest in recent years in tetrahedrally distorted geometries around the Cu(II) ion, particularly because such geometries may be important in the "blue" copper proteins.[1-3] The ternary complex (2,9-dimethyl-1,10-phenanthroline)[glycylglycinato(2–)]copper(II) pentahydrate was synthesized to prepare a copper(II)–peptide complex with such an environment about Cu(II). It was anticipated that the methyl groups on the phenanthroline ring would make four-coordinate square-planar geometry about Cu(II) impossible. Then, if the phenanthroline nitrogen atoms would coordinate instead of the carboxylate oxygen atom, a four-coordinate tetrahedrally distorted complex would result. Some support was provided for this view by the high extinction coefficient of the visible band (ϵ 313 at λ_{max} 633 nm), as compared to the extinction coefficients of Cu(II) complexes with small peptides ($\epsilon \leq 100$). However, the crystal structure determination discussed below shows that the possible steric effects of 2,9-dimethyl-1,10-phenanthroline were accommodated by square-pyramidal coordination, which allowed the carboxylate group to coordinate in the basal plane.

Square-pyramidal coordination is found in many copper(II)–peptide complexes.[4-7] The attractiveness of this geometry for copper(II)–protein–substrate interactions was pointed out by Freeman.[5] The presence of an open axial position may allow the approach of substrate, leading to tetragonally elongated octahedral coordination in the transition state, followed by the breaking of the former axial bond.

Experimental Section

Cupric perchlorate hexahydrate, 99.9% (Gallard-Schlessinger), glycylglycine (gg) (Aldrich), and 2,9-dimethyl-1,10-phenanthroline (dmp), 99% (Aldrich), were used. All other chemicals were of reagent grade quality. The electronic absorption spectrum was obtained using a Beckman ACTA CIII spectrophotometer. The magnetic moment was measured by the Evans method[8,9] with coaxial NMR tubes on a Varian XL-100 NMR spectrometer. X-band EPR spectra were obtained with a Varian Model E-4 EPR spectrometer and were recorded at 9.52 GHz at 25 °C and 9.08 GHz at 77 K. Other experimental conditions were similar to those previously described.[10]

Preparation of (2,9-Dimethyl-1,10-phenanthroline)(glycylglycinato)copper(II) Pentahydrate. $Cu(ClO_4)_2\cdot 6H_2O$, gg, and dmp were combined in stoichiometric amounts in basic solution. Some $Cu(dmp)_2ClO_4$ (red crystalline precipitate) was filtered off after 1 day. During the following week, large deep blue crystals of $Cu(gg)(dmp)\cdot 5H_2O$ formed from solution. These were isolated by suction filtration, washed with 95% ethanol, and air-dried to prevent loss of water of hydration.

Magnetic Moment. The magnetic moment of $Cu(gg)(dmp)\cdot 5H_2O$ was determined by the Evans method, using a 6%-by-weight solution of tetramethylammonium chloride in methanol-d_4, the reference solvent.[8,9] The magnetic susceptibility of the complex, uncorrected for diamagnetism, is given by

$$10^6\chi = \frac{3\Delta f}{2\pi f}\frac{M}{c}$$

where M = molecular weight of the complex, c = concentration of solution (g/mL), f = field strength (Hz), and Δf = shift in the tetramethylammonium chloride signal due to the presence of the paramagnetic ion (Hz). The magnetic susceptibility of the complex was measured at 24.5 and at 55 °C. Diamagnetic corrections were made using Pascal's constants.[11] The magnetic moments, obtained from

$$\mu = 2.829(T\chi)^{1/2}$$

are 2.04 at 24.5 °C and 2.01 at 55 °C.

Electronic and EPR Spectra. The electronic spectrum of a Nujol mull dispersion of $Cu(gg)(dmp)\cdot 5H_2O$ has a broad absorption maximum at about 630 nm. The electronic spectrum of a freshly prepared 10^{-3} M solution of the complex in methanol also has its maximum absorption in this region (ϵ 313 at λ_{max} 633 nm). The intensity of this band decreases over a period of time as the blue solution eventually becomes yellow by the dmp-promoted reduction of Cu(II) to form the stable $Cu^I(dmp)_2^+$ complex ion.[12] The appearance of a new band in the spectrum at 450 nm, attributable to Cu(I) → dmp charge transfer,[13] provides support that the reduction occurs.

In the crystal structure of $Cu(gg)\cdot 3H_2O$,[14] Cu(II) is coordinated by the α-amino nitrogen, the amide nitrogen, the carbonyl oxygen, and a water oxygen in an approximate basal plane, with a second water oxygen coordinating at an apical position. The reported extinction coefficients for this compound are 100 at λ_{max} 635 nm,[15] and 90 at λ_{max} 645 nm.[16] More comparable to Cu(gg)(dmp) are the ternary complexes Cu(gg)(bpy) (bpy = 2,2′-bipyridine) and Cu(gg)(phen) (phen = 1,10-phenanthroline), both of which have extinction coefficients of about 100.[7] Because the extinction coefficient of Cu(gg)(dmp) is three times higher, a particularly distorted geometry was expected around the Cu(II) ion.

Because the d^9 configuration does not have cubic symmetry, a variety of geometries is possible around Cu(II).[17,18] The dominating feature of the coordination environment of Cu(II) in its peptide complexes is a tetrahedrally distorted square-planar base. Usually Cu(II), which may have one or two axial ligands, is displaced from this basal plane by a small amount,[4] 0.254 Å in the case of $Cu(gg)(dmp)\cdot 5H_2O$ (see Crystallographic Results and Discussion). In

0020-1669/78/1317-1429$01.00/0

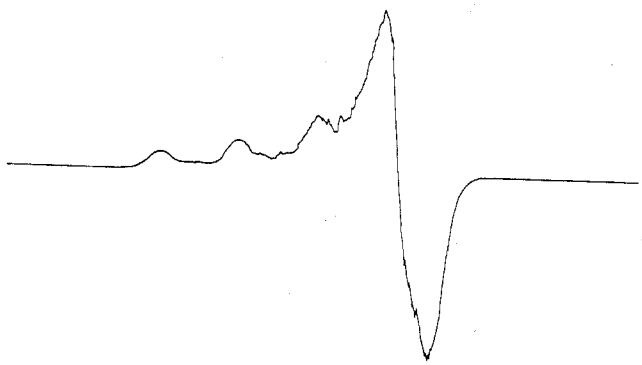

Figure 1. ESR X-band spectrum of a 10^{-3} M solution of Cu(gg)(dmp) in methanol at 77 K (1 cm = 160 G).

contrast, the metal ion is only 0.146 Å out of the plane in Cu(gg)(phen)·$3H_2O$.

The X-band EPR spectrum of a freshly prepared 10^{-3} M solution of the complex was measured in methanol at 25 °C and at 77 K (Figure 1). A complex hyperfine splitting pattern due to nitrogen nuclei is seen in the high-field region. This indicates that, in addition to the three nitrogens in the basal plane, one nitrogen atom coordinates axially.[19] The following values were obtained for the frozen solution: $g_{\parallel} = 2.230$, $g_{\perp} = 2.064$, $|A_{\parallel}| = 16.3 \times 10^{-3}$ cm^{-1}. These values are comparable to the EPR parameters of most copper(II)–peptide complexes.[20-22]

It has been suggested that the mean value of g decreases as the in-plane ligand field increases or as the axial ligand field decreases.[21] A corresponding blue shift of the d–d transitions is expected.[23] Yokoi and co-workers[22] plotted the mean value of the gyromagnetic ratio, g_0, against the wavelength of maximum absorption, λ_{max}, for eight Cu(II) complexes of amino acids, those whose crystal structures were known, and found a linear relation between g_0 and λ_{max}. (Six of these complexes are square pyramidal, one is octahedral, and one is square planar.) The value of g_0 is given by $(g_{\parallel} + 2g_{\perp})/3$ in square-pyramidal geometry and is equal to 2.12 for Cu(gg)(dmp)·$5H_2O$. Its absorption maximum occurs at 15 800 cm^{-1}, and when this point is plotted on Yokoi's approximate straight-line graph, it is seen that Cu(gg)(dmp) falls below the line, indicating stronger axial bonding in Cu(gg)(dmp)·$5H_2O$ as compared to copper(II)–peptide complexes with axial water molecules. In support of this, the copper(II)–apical N bond distance in this complex is shorter than the one in Cu(gg)(phen)[7] (see Crystallographic Results and Discussion). However, no EPR data have been reported for Cu(gg)(phen), so a direct comparison cannot be made.

Diffraction Section. A single crystal of $CuC_{18}H_{18}N_4O_3 \cdot 5H_2O$, an approximately rectangular prism with extreme dimensions 0.26 × 0.20 × 0.22 mm, was selected for x-ray diffraction study and was mounted approximately along its longest dimension.

A Syntex four-circle computer-controlled diffractometer with graphite-monochromatized Mo Kα radiation (Kα_1, λ 0.709 30 Å; Kα_2, λ 0.713 59 Å) was used for preliminary experiments and for the measurement of diffraction intensities. The cell constants and their standard deviations (see Crystal Data) were determined by a least-squares treatment of the angular coordinates of 15 independent reflections with 2θ values up to 22.8° (K$\bar{\alpha}$, λ 0.710 73 Å). The temperature was maintained at 25 (1) °C throughout. The θ–2θ scanning mode was used with a constant scan rate (ω) of 1° min^{-1} (in 2θ). The background time to scan time ratio used was 0.6; the scan range varied from 1.2° at low 2θ to 1.56° at 2θ = 55°. The intensities of three standard reflections, measured after every 100 reflections, showed a small decrease in intensity of about 1.5% during the total data collection, for which the appropriate correction was applied.

Standard deviations were assigned according to the formula

$$\sigma(I) = \{[\mathrm{CT} + (t_c/t_b)^2(B_1 + B_2)]\omega^2 + (pI)^2\}^{1/2}$$

where CT is the total integrated count, B_1 and B_2 are the background counts, t_c/t_b is the scan-time background-time ratio (i.e., 5/3), and the intensity is $I = \omega[\mathrm{CT} - (t_c/t_b)(B_1 + B_2)]$. A value of 0.02 was assigned to the empirical parameter p to account for instrumental inaccuracies. The weights (w) used in least-squares refinement of the structural parameters were the reciprocal squares of $\sigma(F_o)$. Of the 5236 symmetry-independent reflections measured (those for which $3 < 2\theta < 55°$), 4032 had intensities larger than two times their standard deviations, and all but two of these were used in subsequent calculations. The intensities were corrected for Lorentz and polarization effects.[24] The monochromator crystal was assumed to be half perfect and half mosaic in character in the polarization correction. An absorption correction (μ = 11.0 cm^{-1}) was applied[25] which approximated the crystal shape by a 6 × 6 × 6 grid;[26] the calculated transmission coefficients ranged from 0.794 to 0.815. The atomic scattering factors for Cu^+, O^-, O^0, N^0, C^0,[27] and H (bonded)[28] were used, with modifications to the real part of the anomalous dispersion correction[29] for Cu^+.

Crystal Data. (2,9-Dimethyl-1,10-phenanthroline)(glycylglycinato)copper(II) pentahydrate, $CuC_{18}H_{18}N_4O_3 \cdot 5H_2O$, monoclinic, $P2_1/c$, a = 9.591 (4) Å, b = 14.478 (3) Å, c = 17.238 (5) Å, β = 114.79 (2)°, V = 2173 (1) Å^3, formula weight = 491.3, d_{obsd}(flotation) = 1.50 g cm^{-3}, d_{calcd} = 1.502 g cm^{-3}, Z = 4, and $F(000)$ = 1028. The space group was assigned on the basis of the systematic absences, l odd for ($h0l$) and k odd for ($0k0$). Figures in parentheses are estimated standard deviations in the units of the least significant digit given for the corresponding parameter.

Structure Determination. The position of the Cu(II) ion was learned from a three-dimensional Patterson function prepared using the fast-Fourier algorithm.[30] A Fourier function, prepared using phases based on the Cu(II) position, revealed the dimethylphenanthroline (dmp) ligand. A subsequent Fourier function with phases calculated from the copper and dmp atoms indicated the positions of all remaining nonhydrogen atoms, except for those of three water molecules, which were located on a subsequent difference function. After several cycles of both isotropic and anisotropic full-matrix least-squares refinement[31] of the 31 nonhydrogen atoms, all 28 hydrogen atoms were located on a Fourier difference synthesis. Finally, three cycles of least-squares refinement with anisotropic thermal parameters for the nonhydrogen atoms and isotropic thermal parameters for the hydrogen atoms led to the final error indices $R_1 = \sum||F_o| - |F_c||/\sum F_o = 0.038$ and $R_2 = [\sum w(F_o - |F_c|)^2/\sum wF_o^2]^{1/2} = 0.037$. The "goodness-of-fit", $[\sum w(F_o - |F_c|)^2/(m - s)]^{1/2}$, is 1.81. The number of observations used in least-squares is m (4030), and s (392) is the total number of parameters. The overdetermination ratio (m/s) is therefore 10.3. In the final cycle of least-squares refinement, the largest shifts in a nonhydrogen positional or vibrational parameter were 39 and 47% of their corresponding esd's, respectively; for a hydrogen atom, these were 202 and 64%, respectively. The largest peak on the final difference function, whose esd is 0.073 e Å^{-3}, was 0.4 e Å^{-3} in height and was located very near the Cu(II) ion at a chemically implausible position. The positional and thermal parameters of the atoms are given in Tables I and II. Bond lengths and angles are given in Table III.

Crystallographic Results and Discussion

The molecular structure of (2,9-dimethyl-1,10-phenanthroline)(glycylglycinato)copper(II), is presented in Figure 2. The tridentate glycylglycinato (gg) ligand and the bidentate 2,9-dimethyl-1,10-phenanthroline (dmp) ligand coordinate to Cu(II) to form a distorted square pyramid whose base contains the three gg donor atoms and one dmp nitrogen atom. The Cu(II) ion is 0.25 Å above the approximate basal plane (plane IX of Table IV), toward the apical dmp nitrogen atom. The atoms of the equatorial plane show deviations from −0.08 to 0.14 Å in the pattern of a small tetrahedral distortion of the approximately square-planar base. This is a common feature of copper(II)–small peptide complexes and has been discussed by Freeman.[4] Two observations can be made from an examination of Table V. All of the Cu^{II}(gg) complexes listed except Cu(gg)(phen) (phen = 1,10-phenanthroline) and Cu(gg)(dmp) are tetrahedrally distorted, such that the amino nitrogen and carboxylate oxygen atoms are on the same side of the approximate basal plane as Cu(II), whereas in the aforementioned complexes, the reverse situation occurs. Also, the Cu(II) ion is further from its least-squares equatorial plane in Cu(gg)(dmp) than it is in any of the other complexes listed.

The axial Cu(II)–N bond length, 2.263 (2) Å, is shorter than the value reported by Lim, Sinn, and Martin,[7] 2.275 (5) Å, for the corresponding bond in the similar complex Cu-

Table I. Fractional Atomic Coordinates and Thermal Parameters for the Nonhydrogen Atoms, with Estimated Standard Deviations (all ×10^4)[a]

Atom	x	y	z	β_{11}	β_{22}	β_{33}	β_{12}	β_{13}	β_{23}
Cu(1)	4091.4 (3)	1056.8 (2)	2136.1 (2)	80.8 (4)	23.6 (1)	17.0 (1)	−4.8 (4)	29.7 (3)	0.0 (2)
N(2)	5183 (2)	−137 (1)	1747 (1)	77 (3)	27 (1)	19.6 (8)	5 (3)	32 (2)	2 (1)
C(3)	6461 (3)	−622 (2)	2171 (2)	87 (3)	30 (1)	30 (1)	5 (3)	50 (3)	7 (2)
C(4)	7443 (5)	−357 (3)	3073 (2)	119 (5)	55 (2)	34 (1)	57 (6)	8 (4)	4 (3)
C(5)	6891 (3)	−1352 (2)	1778 (2)	104 (4)	31 (1)	45 (1)	25 (4)	67 (4)	6 (2)
C(6)	6015 (3)	−1573 (2)	956 (2)	138 (5)	28 (1)	47 (2)	3 (4)	104 (5)	−13 (2)
C(7)	4658 (3)	−1075 (2)	487 (2)	117 (4)	28 (1)	33 (1)	−33 (4)	77 (3)	−15 (2)
C(8)	3676 (4)	−1254 (2)	−388 (2)	161 (5)	42 (2)	37 (1)	−53 (5)	94 (5)	−36 (2)
C(9)	2407 (4)	−741 (2)	−810 (2)	136 (5)	56 (2)	22 (1)	−72 (5)	48 (4)	−27 (2)
C(10)	1998 (3)	−5 (2)	−391 (2)	92 (4)	44 (2)	21 (1)	−45 (4)	29 (3)	0 (2)
C(11)	715 (3)	567 (2)	−800 (2)	101 (4)	66 (2)	20 (1)	−47 (5)	6 (4)	10 (2)
C(12)	398 (3)	1249 (2)	−362 (2)	85 (4)	54 (2)	32 (1)	8 (4)	14 (4)	28 (2)
C(13)	1352 (3)	1395 (2)	509 (2)	81 (3)	37 (1)	31 (1)	6 (4)	40 (3)	24 (2)
C(14)	1019 (5)	2124 (3)	1013 (3)	126 (5)	40 (2)	46 (2)	52 (5)	70 (5)	18 (3)
N(15)	2599 (2)	870 (1)	910 (1)	70 (3)	27 (1)	21.0 (8)	0 (3)	29 (2)	5 (1)
C(16)	2931 (3)	181 (2)	474 (1)	76 (3)	30 (1)	21 (1)	−23 (3)	36 (3)	0 (2)
C(17)	4294 (3)	−362 (2)	919 (1)	83 (3)	26 (1)	23 (1)	−16 (3)	46 (3)	−1 (2)
O(18)	5065 (2)	2206 (1)	1896 (1)	129 (3)	32 (1)	26.3 (8)	−20 (3)	56 (3)	8 (1)
C(19)	6113 (3)	2580 (2)	2562 (2)	97 (4)	26 (1)	37 (1)	4 (3)	73 (4)	−3 (2)
O(20)	6837 (2)	328 (1)	2542 (1)	142 (3)	30 (1)	57 (1)	−36 (3)	103 (3)	1 (2)
C(21)	6476 (3)	2111 (2)	3410 (2)	91 (4)	32 (1)	29 (1)	−24 (4)	47 (3)	−13 (2)
N(22)	5333 (2)	1403 (1)	3284 (1)	85 (3)	28 (1)	21.1 (8)	−24 (3)	38 (3)	−4 (1)
C(23)	5053 (3)	1080 (2)	3911 (1)	74 (3)	30 (1)	21.3 (9)	18 (3)	34 (3)	3 (2)
O(24)	5749 (2)	1280 (1)	4694 (1)	91 (2)	51 (1)	18.6 (7)	−1 (3)	29 (2)	−3 (1)
C(25)	3763 (3)	379 (2)	3635 (2)	102 (4)	39 (2)	24 (1)	−12 (4)	40 (3)	14 (2)
N(26)	2931 (3)	326 (2)	2699 (1)	88 (3)	26 (1)	24.6 (9)	−7 (3)	35 (3)	−1 (2)
O(27)	8813 (3)	4083 (2)	423 (2)	88 (3)	51 (2)	46 (1)	6 (4)	33 (3)	5 (2)
O(28)	9239 (3)	3258 (2)	2074 (2)	142 (4)	98 (2)	55 (2)	57 (5)	102 (4)	43 (3)
O(29)	3727 (3)	3338 (2)	431 (2)	124 (4)	66 (2)	36 (1)	41 (4)	68 (3)	37 (2)
O(30)	10331 (3)	1463 (2)	2792 (2)	210 (5)	75 (2)	38 (1)	76 (5)	81 (4)	16 (3)
O(31)	775 (3)	3957 (2)	−485 (1)	125 (4)	60 (1)	35 (1)	30 (4)	54 (3)	10 (2)

[a] See Figure 2 for the identities of the atoms. The estimated standard deviations are in the units of the least significant digit given for the corresponding parameter. The anisotropic temperature factor is $\exp[-(\beta_{11}h^2 + \beta_{22}k^2 + \beta_{33}l^2 + \beta_{12}hk + \beta_{13}hl + \beta_{23}kl)]$.

Table II. Fractional Atomic Coordinates and Thermal Parameters for the Hydrogen Atoms, with Estimated Standard Deviations (all ×10^3)[a]

Atom	x	y	z	B, Å^2	Atom	x	y	z	B, Å^2
H(4A)	763 (5)	24 (3)	307 (3)	9.2 (14)	H(25A)	307 (3)	56 (2)	390 (2)	3.7 (6)
H(4B)	708 (6)	−50 (4)	338 (3)	10.4 (18)	H(25B)	420 (3)	−18 (2)	383 (2)	3.9 (7)
H(4C)	831 (5)	−61 (3)	324 (2)	6.9 (11)	H(26A)	288 (3)	−16 (2)	256 (2)	3.7 (8)
H(5)	784 (4)	−163 (2)	207 (2)	4.6 (7)	H(26B)	205 (3)	58 (2)	255 (2)	2.8 (6)
H(6)	630 (3)	−199 (2)	70 (2)	2.8 (6)	H(27A)	791 (5)	395 (2)	19 (2)	5.2 (10)
H(8)	394 (3)	−173 (2)	−65 (2)	4.5 (7)	H(27B)	889 (6)	449 (3)	43 (3)	5.8 (17)
H(9)	187 (3)	−83 (2)	−132 (2)	3.7 (6)	H(28A)	841 (4)	325 (3)	212 (2)	6.0 (10)
H(11)	15 (3)	50 (2)	−135 (2)	3.9 (7)	H(28B)	903 (5)	342 (3)	167 (3)	6.5 (15)
H(12)	−47 (3)	165 (2)	−63 (2)	4.3 (7)	H(29A)	408 (4)	309 (2)	77 (2)	3.1 (9)
H(14A)	14 (5)	237 (3)	71 (3)	8.0 (13)	H(29B)	436 (4)	348 (2)	23 (2)	4.7 (8)
H(14B)	92 (5)	190 (3)	142 (3)	7.8 (14)	H(30A)	1001 (5)	202 (4)	261 (3)	8.8 (14)
H(14C)	171 (5)	254 (3)	123 (3)	7.4 (13)	H(30B)	1045 (5)	151 (3)	320 (3)	6.7 (14)
H(21A)	645 (3)	257 (2)	377 (2)	3.0 (6)	H(31A)	158 (4)	373 (2)	−19 (2)	4.5 (10)
H(21B)	746 (3)	183 (2)	358 (1)	2.3 (5)	H(31B)	34 (4)	393 (3)	−29 (2)	4.5 (11)

[a] See Figure 2 for the identities of the atoms. The estimated standard deviations are in units of the least significant digit given for the corresponding parameter.

(gg)(phen). This effect is a consequence of the increase of steric strain induced in the gg framework, principally by the C(4) methyl group of the dmp moiety (see Figure 2). The steric repulsion between the C(4) methyl group and the amide nitrogen, N(22), induces a warping effect in the gg framework which causes, among other things, a decrease in the axial Cu(1)–N(2) bond distance as compared to Cu(gg)(phen).[7] Another aspect of the induced steric strain is the staggered conformation adopted by the C(4) methyl hydrogens with respect to the amide nitrogen (see Figure 2). The deviation of the C(4) atom from the dmp plane (plane V of Table IV) is also indicative of this effect. However, the C(14) methyl hydrogens, which are farther from the amide nitrogen than those around C(4), adopt the eclipsed conformation with respect to H(12).

The glycylglycine dianion, which is normally quite planar, is markedly nonplanar in this complex. The interplanar angle between the two five-membered chelate rings in Cu(gg) is 17.4°, as compared to 12.8° in Cu(gg)(phen). The dmp moiety is also slightly distorted; the angle between the two C_5N fragments is 2.4°, and the N(2)–C(17)–C(16)–N(15) torsion angle is 1.3°. The pattern of unequal bond distances and angles observed in one end ring of the phenanthroline system is accurately repeated in the other.

The intraligand gg and dmp bond lengths reported here are very similar to those found in other Cu(II) phen or gg complexes.

A few small differences, however, are noted in the coordination distances as compared to other complexes. The copper(II)–amino nitrogen bond length of 2.050 Å is somewhat greater than that reported for Cu(gg)·3H$_2$O[14] (2.02 Å), Cu(gg)(H$_2$O)(9-methyladenine)·4H$_2$O[33] (2.023 Å), Cu(gg)(phen)·3H$_2$O[7] (2.040 Å), Cu(gg)·2H$_2$O[34] (2.030 Å), Cu(gg)(cytosine) (2.011 Å),[35] and Cu(gg)(H$_2$O)(imidaz-

Table III. Molecular Dimensions and Esd's[a]

A. Bond Lengths, Å

Cu(1)-N(2)	2.263 (2)	O(18)-C(19)	1.286 (3)
Cu(1)-N(15)	2.013 (2)	C(19)-O(20)	1.239 (3)
Cu(1)-O(18)	2.033 (2)	C(19)-C(21)	1.514 (4)
Cu(1)-N(22)	1.900 (2)	C(21)-N(22)	1.449 (3)
Cu(1)-N(26)	2.050 (2)	N(22)-C(23)	1.305 (3)
N(2)-C(3)	1.334 (3)	C(23)-O(24)	1.263 (3)
C(3)-C(5)	1.407 (4)	C(23)-C(25)	1.514 (4)
C(5)-C(6)	1.349 (4)	C(25)-N(26)	1.471 (3)
C(6)-C(7)	1.409 (4)	C(4)-H(4A)	0.88 (5)
C(7)-C(17)	1.400 (3)	C(4)-H(4B)	0.78 (5)
N(2)-C(17)	1.360 (3)	C(4)-H(4C)	0.84 (4)
C(16)-C(17)	1.440 (3)	C(14)-H(14A)	0.86 (5)
C(7)-C(8)	1.427 (4)	C(14)-H(14B)	0.81 (5)
C(3)-C(4)	1.491 (4)	C(14)-H(14C)	0.85 (4)
C(13)-N(15)	1.339 (3)	C(5)-H(5)	0.93 (3)
C(12)-C(13)	1.408 (4)	C(6)-H(6)	0.86 (3)
C(11)-C(12)	1.354 (4)	C(8)-H(8)	0.91 (3)
C(10)-C(11)	1.403 (4)	C(9)-H(9)	0.82 (3)
C(10)-C(16)	1.407 (3)	C(11)-H(11)	0.88 (3)
N(15)-C(16)	1.365 (3)	C(12)-H(12)	0.96 (3)
C(8)-C(9)	1.349 (4)	C(21)-H(21A)	0.92 (3)
C(9)-C(10)	1.431 (4)	C(21)-H(21B)	0.96 (2)
C(13)-C(14)	1.484 (5)	C(25)-H(25A)	0.99 (3)
O(27)-H(27A)	0.81 (4)	C(25)-H(25B)	0.92 (3)
O(27)-H(27B)	0.60 (4)	N(26)-H(26A)	0.74 (3)
O(28)-H(28A)	0.83 (4)	N(26)-H(26B)	0.86 (3)
O(28)-H(28B)	0.67 (4)	O(24)-O(29)	2.784 (4)
O(29)-H(29A)	0.64 (3)	O(24)-O(27)	2.720 (4)
O(29)-H(29B)	0.84 (3)	O(20)-O(28)	2.743 (4)
O(30)-H(30A)	0.87 (5)	O(27)-O(28)	2.952 (4)
O(30)-H(30B)	0.66 (4)	O(28)-O(30)	2.879 (5)
O(31)-H(31A)	0.79 (4)	O(29)-O(31)	2.750 (4)
O(31)-H(31B)	0.64 (4)	O(18)-O(29)	2.828 (3)

B. Bond Angles, Deg

N(2)-Cu(1)-O(18)	104.80 (7)	O(28)-H(30A)-O(30)	174 (4)
N(2)-Cu(1)-N(22)	110.14 (8)	O(29)-H(31A)-O(31)	169 (3)
N(2)-Cu(1)-N(26)	99.02 (8)	O(24)-H(29B)-O(29)	175 (3)
N(2)-Cu(1)-N(15)	78.47 (7)	O(24)-H(27A)-O(27)	175 (4)
N(15)-Cu(1)-O(18)	94.66 (7)	C(4)-C(3)-C(5)	120.7 (3)
N(15)-Cu(1)-N(22)	171.22 (8)	N(2)-C(3)-C(5)	121.3 (2)
N(15)-Cu(1)-N(26)	98.02 (9)	N(2)-C(3)-C(4)	118.0 (3)
O(18)-Cu(1)-N(26)	154.82 (8)	C(3)-C(5)-C(6)	120.3 (3)
O(18)-Cu(1)-N(22)	81.67 (8)	C(5)-C(6)-C(7)	120.0 (3)
N(22)-Cu(1)-N(26)	82.58 (9)	C(8)-C(7)-C(17)	119.7 (2)
Cu(1)-N(2)-C(17)	109.3 (1)	C(8)-C(7)-C(6)	123.7 (3)
Cu(1)-N(2)-C(3)	132.3 (2)	C(6)-C(7)-C(17)	116.6 (2)
C(3)-N(2)-C(17)	118.5 (2)	C(9)-C(8)-C(7)	121.1 (3)
C(13)-N(15)-Cu(1)	123.7 (2)	C(8)-C(9)-C(10)	120.9 (3)
C(16)-N(15)-Cu(1)	116.7 (2)	C(9)-C(10)-C(16)	119.4 (2)
O(18)-N(15)-Cu(1)	42.94 (5)	C(11)-C(10)-C(16)	117.0 (2)
Cu(1)-N(15)-C(13)	123.7 (2)	C(9)-C(10)-C(11)	123.6 (3)
N(26)-N(15)-Cu(1)	41.45 (6)	C(10)-C(11)-C(12)	120.3 (3)
N(26)-N(15)-O(18)	82.53 (7)	C(11)-C(12)-C(13)	120.5 (3)
C(13)-N(15)-C(16)	119.6 (2)	C(12)-C(13)-C(14)	121.8 (3)
Cu(1)-O(18)-C(19)	114.6 (2)	C(12)-C(13)-N(15)	120.4 (2)
O(20)-C(19)-C(21)	119.3 (2)	C(14)-C(13)-N(15)	117.8 (2)
O(18)-C(19)-O(20)	123.9 (2)	N(15)-C(16)-C(10)	122.2 (2)
O(18)-C(19)-C(21)	116.8 (2)	N(15)-C(16)-C(17)	118.4 (2)
C(19)-C(21)-N(22)	108.6 (2)	C(10)-C(16)-C(17)	119.5 (2)
Cu(1)-N(22)-C(21)	116.6 (2)	C(16)-C(17)-C(7)	119.5 (2)
Cu(1)-N(22)-C(23)	120.7 (2)	C(16)-C(17)-N(2)	117.2 (2)
C(21)-N(22)-C(23)	127.3 (2)	C(7)-C(17)-N(2)	123.3 (2)
C(25)-C(23)-O(24)	119.1 (2)	H(4A)-C(4)-H(4B)	115 (5)
N(22)-C(23)-C(25)	113.9 (2)	C(3)-C(4)-H(4C)	110 (3)
N(22)-C(23)-O(24)	127.0 (2)	C(3)-C(4)-H(4B)	112 (4)
N(26)-C(25)-C(23)	112.1 (2)	C(3)-C(4)-H(4A)	107 (3)
Cu(1)-N(26)-C(25)	109.8 (2)	H(4A)-C(4)-H(4C)	105 (4)
O(20)-O(28)-O(27)	119.0 (1)	H(4B)-C(4)-H(4C)	108 (5)
O(20)-O(28)-O(30)	94.8 (1)	H(5)-C(5)-C(3)	119 (2)
O(27)-O(28)-O(30)	131.1 (1)	H(5)-C(5)-C(6)	120 (2)
O(18)-O(29)-O(31)	132.4 (1)	C(5)-C(6)-H(6)	121 (2)
O(18)-H(29A)-O(29)	175 (4)	H(6)-C(6)-C(7)	119 (2)
O(20)-H(28A)-O(28)	165 (4)	C(7)-C(8)-H(8)	118 (2)
O(27)-H(28B)-O(28)	168 (5)	C(9)-C(8)-H(8)	121 (2)
		C(8)-C(9)-H(9)	121 (2)

Table V. Results for $F_5X-O-XF_5$ (r_α^0 Values)

	F_5SOSF_5		$F_5SeOSeF_5$		$F_5TeOTeF_5$	
(a) Independent Geometric Parameters and Mean-Square Amplitudes						
X–O, Å	1.586 (11)		1.697 (13)		1.832 (12)	
$(X-F)_{av}$, Å	1.560 (4)		1.681 (3)		1.816 (4)	
$(X-F)_{eq}$, Å	1.558 (8)		1.683 (9)		1.820 (10)	
$(X-F)_{ax}$, Å	1.572 (34)		1.665 (31)		1.799 (47)	
∠XOX, deg	142.5 (1.6)		142.4 (1.9)		145.5 (2.1)	
$\angle F_{ax}XF_{eq}$, deg	87.9 (0.9)		88.9 (0.8)		89.8 (0.9)	
$l(X-F)$,[a] Å	0.043 (3)		0.052 (3)		0.057 (4)	
R_{50}[b]	5.8		4.7		5.6	
R_{25}[b]	7.8		9.1		12.0	
(b) Dependent Interatomic Distances and Mean-Square Amplitudes (Å)						
$F_1 \cdots F_2$	2.17 (3)		2.35 (3)		2.56 (4)	
$F_2 \cdots F_4$	2.20 (1)	0.054 (7)	2.38 (1)	0.084 (6)	2.57 (1)	0.091 (4)
$O \cdots F_2$	2.26 (1)		2.41 (1)		2.59 (2)	
$F_2 \cdots F_3$	3.11 (2)	0.049 (15)	3.37 (2)	0.091 (20)	3.64 (2)	0.055 (20)
$O \cdots F_1$	3.16 (4)		3.36 (3)		3.63 (5)	
$X \cdots X'$	3.00 (3)	0.031 (19)	3.21 (3)	0.056 (6)	3.50 (3)	0.050 (6)
$X \cdots F_3'$	3.11 (3)	0.175 (29)	3.30 (4)	0.179 (25)	3.60 (4)	0.222 (35)
$X \cdots F_2'$	3.73 (2)	0.226 (23)	3.98 (2)	0.237 (35)	4.27 (2)	0.252 (45)
$X \cdots F_1'$	4.52 (4)	0.083 (24)	4.82 (5)	0.091 (21)	5.24 (6)	0.093 (34)
$F_1 \cdots F_3'$	4.37 (5)		4.63 (6)		5.06 (7)	
$F_2 \cdots F_2'$	4.41 (3)	0.314 (64)	4.69 (3)	0.319 (74)	4.99 (4)	0.371 (122)
$F_2 \cdots F_5'$	4.35 (3)		6.63 (3)		5.00 (4)	
$F_3 \cdots F_2'$	3.75 (3)	0.226 (23)	3.97 (4)	0.220 (90)	4.29 (4)	0.147 (43)
$F_2 \cdots F_4'$	3.82 (3)		4.04 (4)		4.28 (4)	
$F_3 \cdots F_3'$	3.26 (4)	0.081 (29)	3.46 (5)	0.100 (*c*)	3.76 (5)	0.100 (*c*)
$F_3 \cdots F_5'$	2.40 (5)		2.51 (6)		2.74 (7)	
$F_1 \cdots F_2'$	5.25 (4)	0.169 (51)	5.59 (4)	0.209 (79)	6.01 (5)	0.173 (76)
$F_1 \cdots F_1'$	5.98 (7)		6.37 (7)		6.94 (10)	

[a] $l(X-O) - l(X-F)$ was assumed. [b] Index of resolution. [c] Assumed.

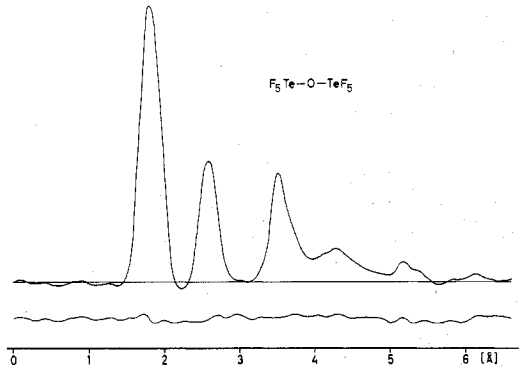

Figure 7. Experimental radial distribution function and difference curve for $(TeF_5)_2O$.

Correlation coefficients >0.6 are listed in Table IV. The mean-square amplitudes are combined into 11 groups according to the respective distances (see Table V). In the final least-squares refinement five geometric parameters and 10 or 11 square amplitudes were refined simultaneously. The results are summarized in Table V; see also Figure 1. The error limits are 3 times the standard deviations.

Discussion

The most interesting geometric parameters for these molecules are the bond angles at the oxygen atom and the eclipsed orientation of the fluorine atoms. The bond angles at the oxygen atom of about 143° for all three compounds are very similar to the value obsevered for siloxane[19] (Si–O–Si = 144.1 (0.9)°). But when silicon is replaced by germanium, the corresponding angle decreases to 126.5 (0.3)°[20] for digermyl ether. Such smaller bond angles are known in FSO_2-O-SO_2F and $FSO_2-O-SO_2-O-SO_2F$[21] (123.6 (1.0) and 123.6 (2.4)°, respectively). There are two possible explanations for the large bond angles in the XF_5-O-XF_5 molecules: (1) steric repulsions between the X atoms or fluorine atoms or (2) partial delocalization of the oxygen lone pairs. Steric repulsions may be seen in $F_5S-O-SF_5$, where the close contact of fluorine atoms on different SF_5 groups is only 2.4 Å. These fluorine atoms are bent 2.1° away from the octahedral orientation, but this effect diminishes in $F_5Se-O-SeF_5$ (1.1°) and disappears in $F_5Te-O-TeF_5$. Steric interaction would cause also lengthening of the X–O bond together with opening of the bond angle, as observed, e.g., for $t\text{-}Bu_3CH_2$[22] or $t\text{-}Bu_3P$,[23] whereas delocalization of the oxygen lone pairs would result in $p_\pi-d_\pi$ contribution to the O–X bond and thus cause shortening of this bond. But unfortunately not many structural data are known for molecules in the gas phase, which can be compared with the X–O bond distances in $F_5X-O-XF_5$.

In the sulfur compound of this investigation the S–O bond is somewhat shorter than in F_5S-OF[24] (r_a(S–O) = 1.64 Å) and $F_5S-O-O-SF_5$[25] (r_a(S–O) = 1.66 (5) Å), but it is considerably longer than the double bonds in SO_2 or SO_3[26] which are r_a(S=O) = 1.431 (2) and 1.418 (3) Å, respectively. A remarkable analogy between the SF_5 and $SiMe_3$ groups is observed when the respective oxides are compared with the peroxides. With a decrease of the bond angle at the oxygen atom from 148 (3)° in the siloxane[27] to 106.6 (1.4)° in the disilyl peroxide[28] the Si–O bond length increases from 1.631 (3) to 1.681 (3) Å. For the corresponding SF_5 compounds the bond angle decreases from 142.5 (1.6)° to 105 (3)° and the S–O bond length increases from 1.586 (11) to 1.66 (5) Å. Although the uncertainties in the S–O bond lengths of F_5S-OF and $F_5SO-OSF_5$ are rather large, this comparison indicates that the large bond angle in F_5SOSF_5 is associated with *a shortening* of the S–O bond.

In the case of selenium no structural data of an analogous molecule with an Se–O single bond are known for the gas phase. For SeO_3 tetramer[29] and ethylene selenite,[30] Se–O single-bond lengths of 1.790 (8) and 1.80 (2) Å have been observed. The Se–O bond distance in $F_5SeOSeF_5$ is between this single-bond value and the double bond in SeO_2[31] (r_g(Se=O) = 1.61 (1) Å). Considerable amount of double-bond contribution has to be assumed also for the tellurium compound. Within the error limits the Te–O bond length in

Table IV. Correlation Coefficients >0.6

	F_5SOSF_5	$F_5SeOSeF_5$	$F_5TeOTeF_5$
r(X-O), ∠XOX	0.82	0.95	0.97
r(X-F_{eq}), r(X-F_{ax})	0.98	0.97	0.98
l(X···X'), l(F_1···F_2)	0.67	0.64	0.73
∠XOX, ∠$F_{eq}XF_{ax}$		0.60	
l(X-F), ∠$F_{eq}XF_{ax}$		0.65	
r(X-F_{eq}), l(X-F)	0.67		
r(X-F_{eq}), l(F_2···F_3)	0.68		

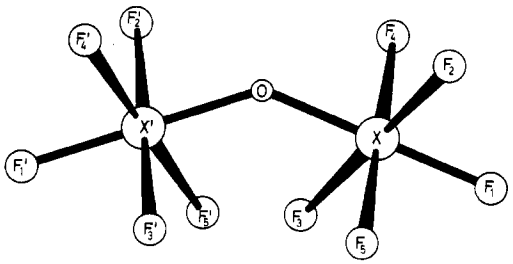

Figure 1. Geometric model for $F_5X-O-XF_5$.

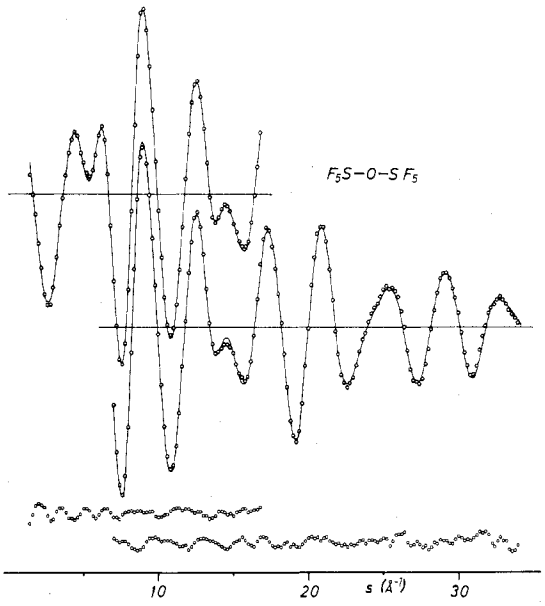

Figure 2. Experimental (O) and theoretical (—) molecular intensities for $(SF_5)_2O$.

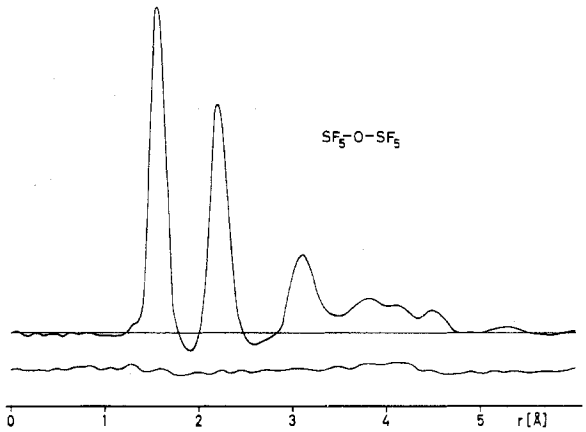

Figure 3. Experimental radial distribution function and difference curve for $(SF_5)_2O$.

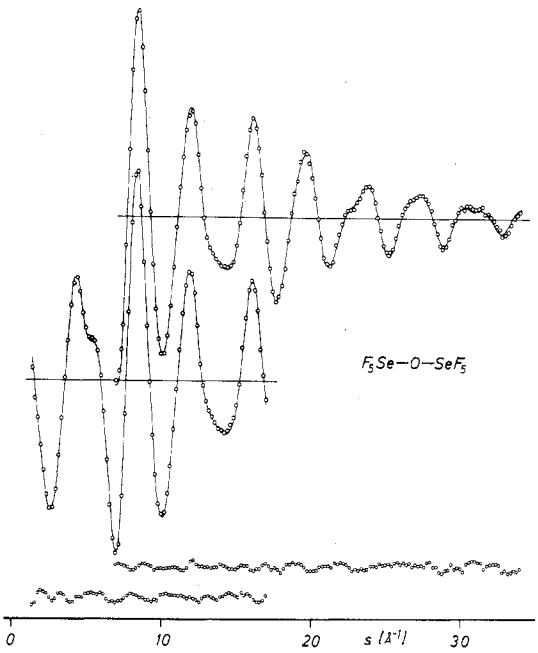

Figure 4. Experimental (O) and theoretical (—) molecular intensities for $(SeF_5)_2O$.

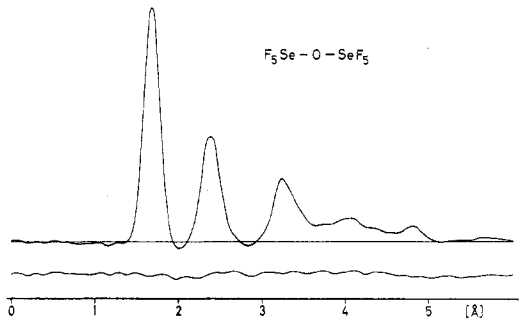

Figure 5. Experimental radial distribution function and difference curve for $(SeF_5)_2O$.

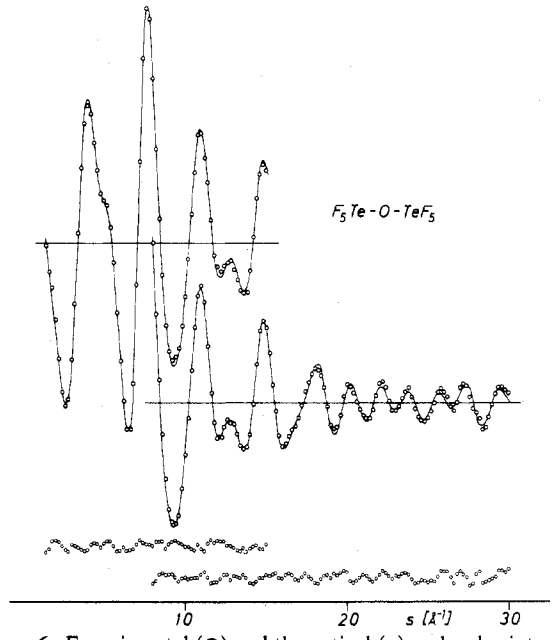

Figure 6. Experimental (O) and theoretical (-) molecular intensities for $(TeF_5)_2O$.

tances agree very well with the respective values for XF_6 molecules (Table VI).

Table I. Details of the Experiment

	Camera distance, cm	T_{sample}, °C	T_{nozzle}, °C	P_{camera}, Torr	Exposure, s	Wavelength, Å	s range, Å^{-1}
F_5SOSF_5	50	−48	10	5×10^{-6}	15-40	0.049 26 (2)	1.4-16.8
	25	−45	10	1×10^{-5}	45-70	0.049 33 (1)	7.0-34.0
$F_5SeOSeF_5$	50	−27	10	2×10^{-6}	45-80	0.049 24 (1)	1.4-17.0
	25	−30	10	5×10^{-6}	120-180	0.049 30 (1)	7.0-34.0
$F_5TeOTeF_5$	50	−36	15	1×10^{-5}	40-70	0.049 31 (1)	1.4-15.0
	25	−32	15	1×10^{-5}	90-180	0.049 32 (1)	8.0-30.0

Table II. Force Constants for Y_2O Skeleton (mdyn Å^{-1}, mdyn, and mdyn Å)

	Y = SF_5	Y = SeF_5	Y = TeF_5
f_r	5.3	4.3	4.4
f_α	2.3	1.5	1.1
f_{rr}	0.8	0.8	0.4
$f_{r\alpha}$[a]	0.1	0.1	0.1

[a] Assumed.

7 g. The purity of these products was monitored by ^{19}F NMR spectroscopy and was always found better than 99%. The diffraction intensities were recorded with a Balzers diffractograph KDG 2[12] for two camera distances (50 and 25 cm). The accelerating voltage was approximately 60 kV and the wavelength was determined from ZnO diffraction patterns. Details of the experiment are summarized in Table I. Kodak electron image plates were used for the sulfur derivative and Ilford N50 plates for the selenium and tellurium compounds. Three plates of each data set were reduced by the usual procedure[13] of this laboratory. For the short camera distance, intensities recorded without gas were subtracted. The background was refined separately for each recording. The averaged molecular intensities $sM(s)^{expl}$ for the two camera distances are presented in Figures 2, 4, and 6.

Vibrational Analysis

The infrared and Raman spectra[9,10] show many low vibrational frequencies for these molecules. Thus, rather large perpendicular mean-square amplitudes are expected which may have a considerable effect on the geometric parameters determined by electron diffraction. To account for these effects, the shrinkage corrections $\Delta r = r_a - r_\alpha{}^0$[14] were estimated from a very crude force field. For the XF_5 groups the force constants of the respective XF_6[15] molecules were transferred. The force constants characterizing the vibrations of the Y_2O molecular skeleton (Y = XF_5) were calculated with a three-mass-model from the frequencies $\nu_s(Y_2O)$, $\nu_a(Y_2O)$, and $\delta(Y_2O)$.[10] The bending vibration for the sulfur compound which is not given in ref 10 was assigned to a very strong raman band at 265 cm^{-1}. The force constants for the Y_2O skeleton are listed in Table II. . From the vibrational spectra no information about the torsion of the XF_5 groups around the O–X bond can be obtained. As was demonstrated in the case of perfluoroneopentane,[16] the torsional motions have a strong effect on the mean-square amplitudes of some nonbonded distances and on the skrinkage corrections for distances which are independent of torsion. For these distances the torsional contributions were neglected. For all three compounds a torsional force constant $f\tau$ = 0.5 mdyn Å was used in the spectroscopic calculations. This value is based on two considerations: (1) the X–O bond distances indicate a considerable double bond character and (2) the effective deviation of the XF_5 groups from the eclipsed position is <4° (see Structure Analysis). The shrinkage corrections calculated with these crude force fields are listed in Table III. The corrections for the Y_2O skeleton are smaller than expected from the vibrational spectra.

Structure Analysis

Preliminary geometric parameters and the orientation of the XF_5 groups around the O–X bond were determined by analyzing the radial distribution functions (Figures 3, 5, and 7). Comparing theoretical radial distribution functions for various models with the experimental function demonstrates that approximate agreement between model and experiment is obtained with a C_{2v} model and dihedral angles $\delta(XOXF_{eq}) \sim 45°$; i.e., the equatorial fluorine atoms are eclipsed. These preliminary models were refined in a least-squares analysis, based on the molecular intensities. The diagonal elements of the weight matrix increased exponentially for $1.4 < s < 4$ Å^{-1} and decreased exponentially for $14 < s < s_{max}$ for the 50-cm data. For the short camera distance the respective ranges were $s_{min} < s < 9$ Å^{-1} and $30 < s < 34$ Å^{-1}. For the 25-cm data of the tellurium compound the weight decreased for $25 < s < 30$ Å^{-1}. For both camera distances an s interval of Δs = 0.2 Å^{-1} was chosen. Scattering amplitudes and phases published by Haase[17] were used in the calculations. For $F_5Te–O–TeF_5$ we also calculated a least-squares refinement with the scattering amplitudes and phases of Schäfer et al.[18] The differences in the geometric parameters were negligible (~0.001 Å for bond distances) and for the mean-square amplitudes the differences were smaller than the error limits. The $r_a - r_\alpha{}^0$ corrections were included in the least-squares procedure. Assuming C_{4v} symmetry for the XF_5 groups, various possible distortions of the $-XF_5$ group were considered: (1) deviation of the angle $F_{ax}XF_{eq}$ from 90°, (2) tilt of the XF_5 group with respect to the O–X bond direction, (3) deviation of the dihedral angle $\delta(XOXF_{eq})$ from 45°. In the last case the XF_5 groups were rotated in opposite directions; i.e., the overall symmetry of the molecule was C_2. Since the distortions (2) and (3) were smaller than the respective error limits for all three molecules, they were not considered in the further calculations. Assuming $(X–F)_{eq} = (X–F)_{ax}$ an average value $(X–F)_{av}$ for this bond length was obtained from a least-squares analysis. Refining the X–F distances separately resulted in high correlations and large standard deviations for these parameters and thus did not lead to any conclusive result because of the large error limits. For the sulfur compound $r_{ax} > r_{eq}$ while for the selenium and tellurium compounds $r_{ax} < r_{eq}$. In all cases, however, the differences between r_{ax} and r_{eq} are smaller than the error limits. The average X–F dis-

Table III. Corrections $\Delta r = r_a - r_\alpha{}^0$ for $(XF_5)_2O$ in Angstrom Units

	F_5SOSF_5	$F_5SeOSeF_5$	$F_5TeOTeF_5$
X–O	0.001	0.001	0.002
X–F	0.002	0.004	0.006
O···F_{ax}	0.002	0.003	0.005
O···F_{eq}	0.000	0.001	0.002
F_{ax}···F_{eq}	0.001	0.001	0.002
F_2···F_3	0.001	0.001	0.003
F_2···F_4	0.000	0.001	0.001
X···X′	0.000	0.000	0.000
X···F_1″	0.001	0.001	0.002
X···F_2′	0.000	0.000	0.000
X···F_3′	0.000	0.000	−0.001
F_1···F_1′	0.001	0.001	0.002
F_1···F_2′	0.000	0.000	0.001
F_1···F_3′	0.001	0.000	0.000
F_2···F_2′	0.000	0.000	−0.001
F_2···F_3′	0.001	0.000	0.000
F_2···F_4′	−0.003	−0.004	−0.004
F_2···F_4′	0.003	0.003	0.003
F_3···F_3′	0.001	0.001	0.000
F_3···F_5′	−0.004	−0.006	−0.007